Vapor Synthesis of Titania Powder by Titanium Tetrachloride Oxidation

M. Kamal Akhtar, Yun Xiong, and Sotiris E. Pratsinis
Dept. of Chemical Engineering, Center for Aerosol Processes, University of Cincinnati, Cincinnati, OH 45221

Formation of titania particles by vapor-phase oxidation of titanium tetrachloride was studied in an aerosol reactor between 1,200 and 1,723 K. The effect of process variables (reactor residence time, temperature, and reactant concentration) on powder size and phase characteristics was investigated using the differential mobility particle sizer, scanning electron microscopy, and X-ray diffraction. Titania particles were primarily anatase though the rutile weight fraction increased with increasing reactor temperature. The geometric number average diameter of the particles was between 0.13 and 0.35 μm, and the geometric standard deviation of the particle size distribution was about 1.4. The average particle size increased with increasing temperature, inlet $TiCl_4$ concentration, and residence time. The observed changes in the particle size distribution were compared with those predicted by solving the aerosol dynamic equation by a sectional method and accounting for coagulation and first-order chemical reaction. While variations in the process variables resulted in discernible changes in the size of the particles, the spread of the distribution remained rather unaffected.

Introduction

Powder preparation is one of the most basic steps for much of pigments manufacture and ceramic processing. The preparation of ceramic powders has been moving increasingly toward a broader diversity of preparation processes with emphasis on more sophisticated chemical processing (Rice, 1990). While chemical and phase composition are basic requirements, control of particle size and morphology is of increasing importance.

Ultrafine titania particles are produced routinely on a large scale by the oxidation of titanium tetrachloride ($TiCl_4$) vapor, the so-called "chloride" process. Reactions in the gas phase in the temperature range 973–1,673 K result in the formation and growth of fine titania particles. Titanium dioxide pigments are used in coatings to provide maximum light scattering with virtually no absorption. The pigmentary properties of titania, for instance, hiding power (opacity) and gloss, are related directly to particle size and polydispersity (Kingery et al., 1976). The light scattering power of titania particles is a strong function of their size and exhibits a maximum between 0.15 and 0.25 μm (Clark, 1975).

Correspondence concerning this article should be addressed to S. E. Pratsinis.

Titania production from titanium tetrachloride vapor has been the focus of experimental studies in the past. Formenti et al. (1972) prepared titania particles from the oxidation of $TiCl_4$ in an oxygen-hydrogen diffusion flame. The particle diameters were in the range of 0.01–0.2 μm, and their geometry and crystalline structure were found to be a function of $TiCl_4$ loading and residence time in the flame. These particles were found to exhibit unusual photocatalytic activity in the oxidation of paraffins and olefins. Investigations into TiO_2 generation by $TiCl_4$ oxidation in premixed flames were conducted by George et al. (1973) who found the product particles to have a self-preserving size distribution. Suyama and Kato (1976) studied titania formation by $TiCl_4$ oxidation in a furnace flow reactor and found from electron microscopic analysis that the particle size decreased with increasing reaction temperature and oxygen concentration and with decreasing $TiCl_4$ concentration. Toyama et al. (1990) produced particles in a similar manner and their results indicated the same temperature dependence as that observed by Suyama and Kato but the median diameter was found to be independent of $TiCl_4$ concentration. Morooka et al. (1987) conducted similar experiments in a two-stage furnace flow reactor and found that the particle size

decreased with increasing temperature in the first reactor but increased with increasing reactor temperature and addition of $TiCl_4$ in the second reactor. Kobata et al. (1991) extended the work of Morooka et al. (1987) and developed a discrete-sectional model including the sintering rate of particles and phase transformation to predict titania particle size and the change of anatase to rutile titania as a function of residence time and reactor temperature. Furthermore, there are several patents dealing with the formation of TiO_2 particles including developments related to reactor design, mixing geometry, and nucleating agents; yet, the fundamentals are still not understood (Bowen, 1980).

In this article a systematic experimental investigation of the formation of titania particles was carried out by the reaction between titanium tetrachloride and oxygen in a tubular aerosol flow reactor at temperatures ranging between 1,200 and 1,723 K. Tubular reactors allow operation under well defined stoichiometries, temperatures and residence times, and provide excellent control of the process variables affecting powder characteristics. Titania was chosen as the model compound for investigation not only because of its bulk use in the pigment industry but also because the reaction kinetics and mechanisms for its formation are reasonably well understood (Pratsinis et al., 1990). The particle size and powder characteristics were studied as a function of temperature, $TiCl_4$ concentration, and reactor residence time. The differential mobility particle size (DMPS) was used as the primary particle characterizing equipment, and the morphology of the particles was obtained from electron microscopy. Detailed particle size distributions obtained from image analysis of scanning electron micrographs were compared to the distributions obtained from the DMPS. The crystal structure and phase composition of the particles were obtained by X-ray diffraction. Experimental observations of the size distribution were compared with theoretical predictions obtained by solving the aerosol dynamic equation using a sectional technique.

Experimental Studies

Apparatus

A schematic of the experimental apparatus is shown in Figure 1a. Clean, dry argon carrier gas (Wright Brothers, 99.8%) is bubbled through a fritted glass outlet into a gas washing bottle (a) containing $TiCl_4$ (Aldrich, 99.9%) at room temperature (≈ 296 K). This bottle is placed on a top loading balance (Fisher XT-100, ± 0.01 g) measuring the entrainment of $TiCl_4$ in the flowing carrier gas during the course of the experiment. The mixture of Ar-$TiCl_4$ is diluted with a controlled amount of additional argon, combined with the appropriate amount of oxygen and introduced into the aerosol reactor (b). It should be noted that since $TiCl_4$ is sensitive to the presence of water, all gases are filtered and passed through silica desiccant (c) (Fisher 09-206, dried to a dew point of 200 K) prior to their use in the experiments. The reactor is a 3.175-cm-ID (3.81-cm-OD), 152.4-cm-long alumina tube (99.8% Al_2O_3, Coors Ceramics Inc.) that is externally heated in a horizontal furnace (d) (Lindberg 54233). The reactor temperature is set and maintained by a temperature controller (Lindberg 59545). The reactor outlet gas stream is rapidly mixed and cooled with nitrogen gas in the primary dilutor (e). The dilutor consists of two concentric tubes: 2.54-cm-OD, 2.06-cm-ID outer tube and 1.27-cm-OD, 0.953-cm-ID inner tube. The entire dilution system is made of Haynes' alloy 214 (Haynes International) that resists degradation by chlorine which is present in the reactor effluents. Cool nitrogen gas comes into the reactor from the outer annulus, mixes with the reactor effluents, and the cooled gases exit the reactor through the inner tube. The primary dilutor quenches chemical reaction and inhibits particle growth by coagulation outside the reaction zone. In addition, it reduces thermophoretic losses from the produce stream onto the cool dilutor walls (Figure 1b). The diluted reactor effluents are sampled by the differential mobility particle sizer, collected on filters, or exhausted through the laboratory hood after scrubbing in a sodium hydroxide solution. All flows into the reactor are precisely controlled using mass flow controllers (f) (1259B, MKS).

Measurements

Detailed temperature measurements were made along the reactor axis as a function of nitrogen flow rate in the absence of reactants. These measurements were made using a copper-constantan thermocouple (K type, Cole-Parmer). Figure 2 shows typical axial temperature profiles in the reactor at different inlet gas flow rates at a set temperature of 1,373 K. The measured temperatures on the inlet side were within 25 K of those predicted by the Graetz solution. During these measurements a flow rate of 10 L/min of nitrogen was maintained in the primary dilution system to assure that the operation of the primary dilutor was accounted for in the actual reactor temperature profiles. At the inlet gas flow rates employed (up to 6L/min), a nearly isothermal zone, 30 cm long, exists. In this zone the temperature remains nearly constant and identical to the furnace set temperature. The reactants are present in dilute concentrations so the released heat of reaction is insufficient to appreciably affect reactor temperature.

The concentration of $TiCl_4$ vapor in the gas stream is determined by recording the weight of the $TiCl_4$ containing bottle before and after each experiment carried out at constant argon flow through the bottle. The change in weight divided by the product of the duration of the experiment and the total gas flow rate into the reactor gives the concentration of $TiCl_4$ vapor in the gas stream at inlet conditions. For calculations and specification of experimental conditions, this concentration is corrected to account for the expansion of gases at the reaction temperatures employed. Table 1 shows the $TiCl_4$ concentration as a function of carrier gas flow rate at 1,400 K. The $TiCl_4$ concentrations at reactor inlet and in the high-temperature reaction zone are also shown.

For particle size distribution measurement, a small stream of the primary dilutor exhaust is withdrawn and further diluted with dried, filtered air in a 50-L polyethylene dilution bottle (g). This secondary dilution was used to further reduce particle concentration so that a differential mobility particle sizer (DMPS, TSI 3932) could be used for real-time measurement of the titania particle size distribution. The DMPS measures particle size distribution by classifying the aerosol on the basis of electrical mobility using a classifier (TSI 3071) and counting the particles using a condensation nucleus counter (TSI 3020). A vacuum pump (j) draws in controlled amounts of diluted reactor effluent and maintains the underpressure necessary for the operation of the particle sizing instruments. The flows into

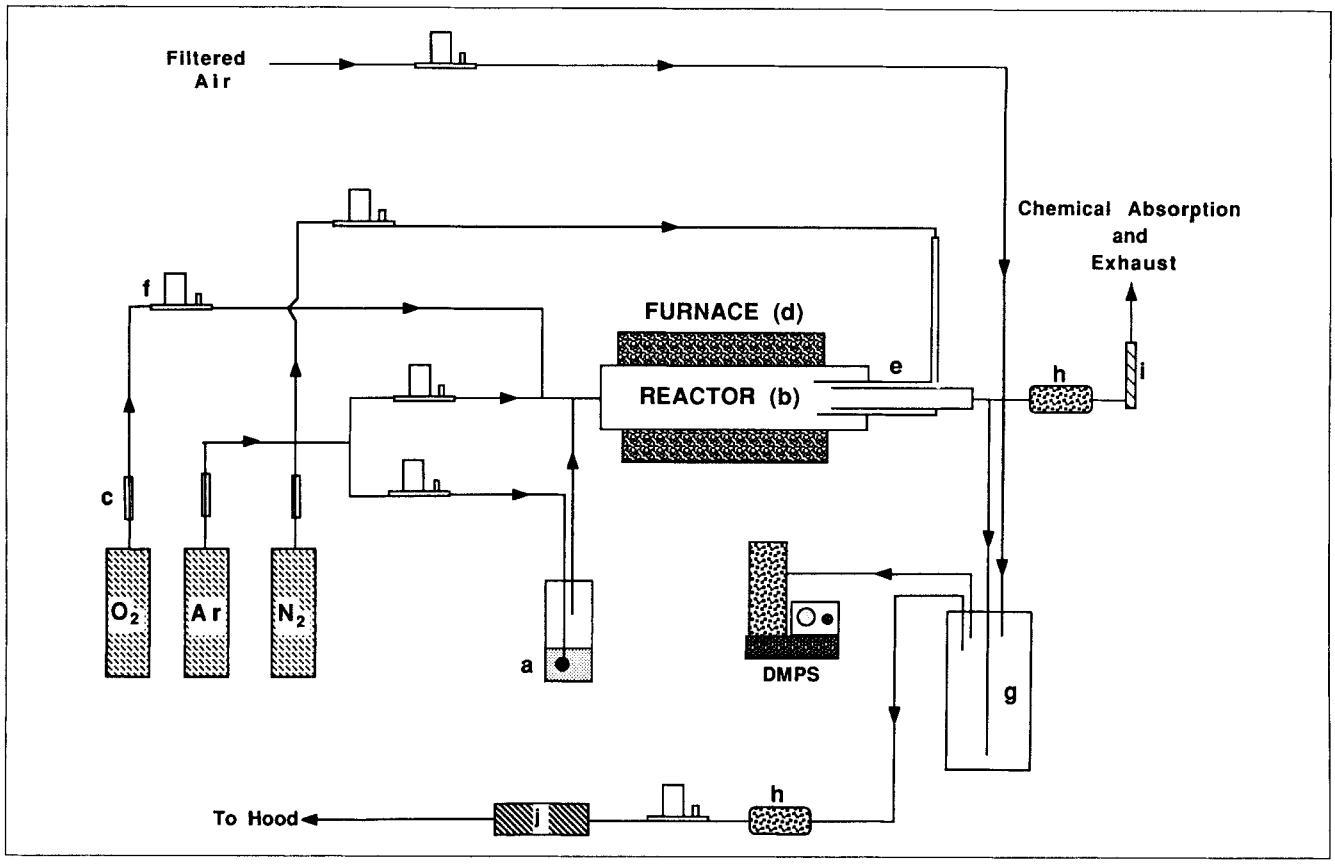

Figure 1a. Experimental apparatus used to produce titania particles from vapor-phase oxidation of titanium tetrachloride.

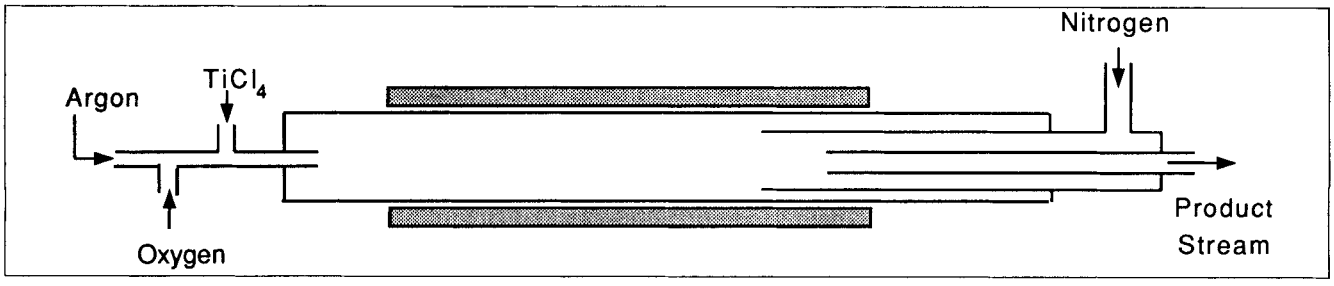

Figure 1b. Reactor showing inlet and outlet arrangements and primary dilutor.

and out of the secondary dilutor are monitored for precise determination of the dilution ratio. The excess reactor effluents are passed through an airline filter (h) (MSA #81857), a rotameter (i) and sodium hydroxide solution (to absorb chlorine) before being exhausted into the laboratory hood. The rotameter provides a check on the stability of flows during the course of the experiment.

Samples for X-ray diffraction were collected on polycarbonate filters (Nuclepore) and those for microscopic analysis on copper grids. The scanning electron micrographs were obtained on a Cambridge (Model 90B) microscope. These micrographs were digitized using a scanner (Scanjet, Hewlett-Packard), and image analysis was done on a Macintosh II computer using Image 1.2b software. The X-ray diffraction patterns were obtained on a Siemens diffractometer (Kristalloflex, D500). The weight fraction of anatase and rutile phases in the samples were calculated from the relative intensities of the strongest peaks corresponding to anatase and rutile as described by Spurr and Myers (1957).

Procedure

The furnace was heated to the desired temperature, the argon flow rate through the $TiCl_4$ containing bottle was maintained constant, and the flow of oxygen was set at the desired level, usually in excess of the stoichiometric amount. The residence time in the reactor was controlled by the upstream dilution argon flow rate. The flow of nitrogen in the primary dilutor was varied between 4 and 6 L/min depending on the temperature at which the reactions were conducted and on the flow rates of the incoming gases. The effluent flow (after primary dilution) into the dilution bottle was maintained between 0.1

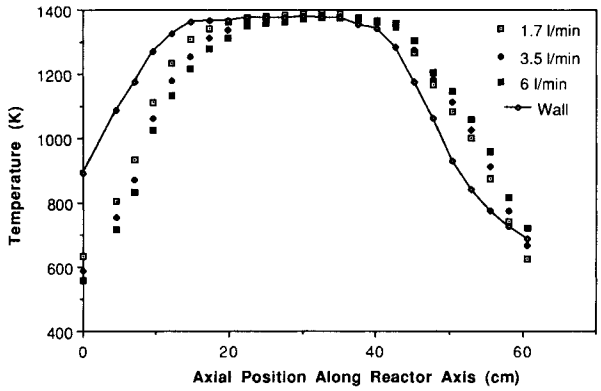

Figure 2. Axial temperature profile along the center line in the reactor at inlet gas flow rates of 1.7, 3.5, and 6 L/min with the furnace set temperature at 1,373 K.

Zero indicates the start of the furnace. The silicon carbide heating elements were placed between 18 and 44 cm from the furnace inlet. The flow in the primary dilutor was 10 L/min.

and 0.2 L/min, and the flow of dry clean air was kept steady at ≈21–23 L/min. It was critical to maintain a steady and consistent flow of reactor effluent into the secondary dilution stage as variations in this flow caused the largest fluctuations in the particle concentration measured by the DMPS. The DMPS was operated in the "underpressure" mode with an inlet flow of polydisperse aerosol sample of 0.3 L/min and sheath air flow of 3.0 L/min. This mode of operation enabled particles between 0.017 and 0.886 μm to be sized.

Theory

Well mixed reactants, $TiCl_4$ and O_2, in argon carrier gas are introduced into the aerosol reactor. Neglecting radial and axial diffusion of $TiCl_4$, a mass balance for $TiCl_4$ can be written as:

$$\frac{dc}{dt} = -k_1(T)c \tag{1}$$

where t is the reactor residence time and k_1 is the Arrhenius reaction rate constant for $TiCl_4$ oxidation. Hence, the $TiCl_4$ concentration along the reactor axis can be written as:

$$C = C(0)\exp\{-k_1(T)t\} \tag{2}$$

where $k_1(T) = k_0 \exp(-E/RT)$. The apparent activation energy for the reaction $E = 88.8 \pm 3.2$ kJ/mol and the preexponential factor $k_0 = 8.29 \times 10^4$ s^{-1} for temperatures between 973 and 1,273 K (Pratsinis et al., 1990).

Formation of titania by $TiCl_4$ oxidation takes place at high temperatures (T = 1,000–2,000 K) by chemical reaction and coagulation, since the thermodynamic critical size of product titania particles is less than that of a single titania molecule (Ulrich, 1971; Xiong and Pratsinis, 1991). Assuming that titania molecules and particles fully coalesce upon colliding and neglecting particle wall losses, titania formation and growth can be described by the coagulation equation for single titania molecules as:

$$\frac{dn_1}{dt} = C(0)Ak_1\exp(-k_1t) - n_1\sum_{j=1}^{\infty}\beta_{i,j}n_j \tag{3}$$

and for all other particles as:

$$\frac{dn_i}{dt} = \frac{1}{2}\sum_{j=1}^{i-1}\beta_{j,i-j}n_jn_{i-j} - n_i\sum_{j=1}^{\infty}\beta_{i,j}n_j \tag{4}$$

where n_i is the concentration of titania particles containing i molecules and $\beta_{i,j}$ is the coagulation coefficient for collision of particles containing i and j titania molecules. The first righthand side term in Eq. 3 accounts for the increment in the concentration of titania molecules due to $TiCl_4$ oxidation, and the first righthand side term in Eq. 4 accounts for increase in the concentration of particles of size i by coagulation of smaller particles. The second righthand side terms in Eq. 3 and 4 account for the loss of monomers and particles of size i, respectively, by coagulation with all particles. The effects of van der Waals forces, electrical forces and particle shape are neglected, since they depend on the employed compound and are hard to estimate from first principles.

In principle, Eq. 3 and a few billion differential equations like Eq. 4 need to be solved simultaneously to describe the dynamics of all particles from molecular clusters to micron-sized particles. Consequently, a straightforward numerical solution (for example, discrete model, Landgrebe and Pratsinis, 1989) quickly runs into formidable computer time requirements. Sectional models overcome the excessive computational demand of discrete models as well as the oversimplification of moment models. Here, the sectional solution to the above equations was used as formulated by Landgrebe and Pratsinis (1990) and Xiong and Pratsinis (1991). Specifically, the particle size domain was divided into a finite number of sections within

Table 1. Concentration of $TiCl_4$ Introduced into the Reactor as a Function of the Carrier Argon Flow Rate

Flow Rate						
Dilution Argon L/min	Oxygen cm^3/min	Carrier Argon to $TiCl_4$ Washing Bottle cm^3/min	$TiCl_4$ Carried mol/min × 10^4	$TiCl_4$ Conc. at Reactor Entrance mol/L × 10^5	$TiCl_4$ Conc. in Reaction Zone at 1,400 K mol/L × 10^6	Res. Time in Heated Section s
2	25	148	1.02	4.7	9.94	1.87
2.5	31	188	1.28	4.7	9.94	1.57
3.5	44	268	1.79	4.7	9.94	1.32
4.5	56	347	2.30	4.7	9.94	0.84

If the flow rate of dilution argon is changed, then the flow of carrier argon needs to be adjusted to maintain constant $TiCl_4$ concentration. Moreover, the concentration of $TiCl_4$ at reactor entrance conditions is higher than that in the reaction zone. The temperature in the reaction zone, for the data shown, was 1,400 K.

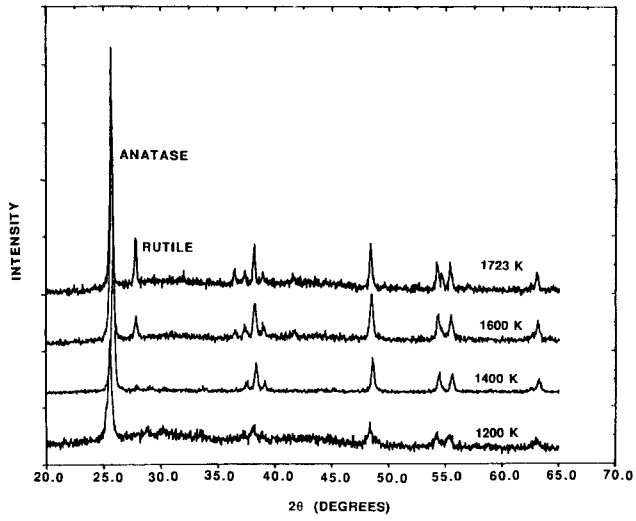

Figure 3. X-ray diffraction patterns for TiO_2 particles at different temperaures at a $TiCl_4$ loading of 1.16×10^{-5} mol/L.

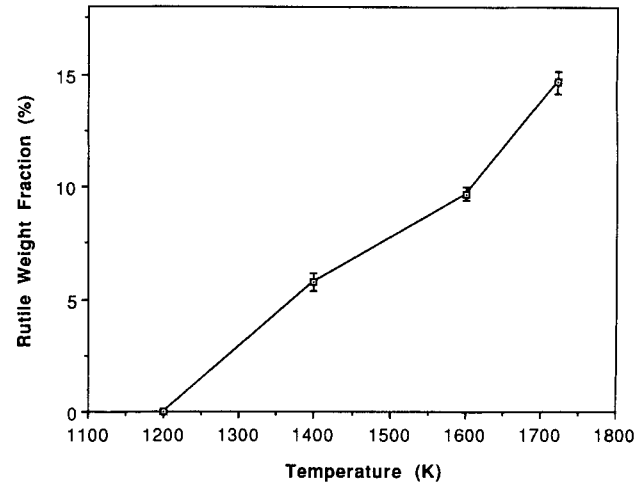

Figure 4. Increase in rutile weight fraction of titania particles as a function of temperature.

These powders were synthesized at a $TiCl_4$ loading of 1.16×10^{-5} mol/L and residence time ≈ 1.6 s.

which the aerosol volume was kept constant (Gelbard et al., 1980). The present formulation of the sectional model gives fairly accurate predictions of the aerosol dynamics (Landgrebe and Pratsinis, 1990).

Results and Discussion

Chemical reaction and coagulation determine the characteristics of the product titania particle size distribution. Consequently, reactor temperature, residence time, and reactant concentration control particle concentration, average size, and polydisperity. Titania particle size distributions were measured at reactor temperatures ranging from 1,200 to 1,723 K, at initial $TiCl_4$ concentrations ranging from 9.34×10^{-6} to 1.56×10^{-5} mol/L and at residence times between 0.8 and 1.6 s. At temperatures greater than 1,200 K a significant amount of a $TiCl_4$ can be converted before the reactants enter the isothermal zone of the reactor. This is taken into account by integrating the conversion equation (Eq. 1) along the nonisothermal temperature profile in the reactor (Figure 2). The residence times reflect the entire time reactants spend at temperatures greater than 500 K. Oxygen used in these experiments was between 5 and 10 times in excess of the stoichiometric amount. Typical flow rates of the dilution argon were between 2 and 5 L/min.

The phase composition of titania powders was obtained from X-ray diffraction (XRD). The XRD patterns for pure titania particles produced at 1,200, 1,400, 1,600 and 1,723 K are shown in Figure 3. The particles produced in these experiments are primarily anatase, though the rutile phase is also observed at temperatures in excess of 1,200 K. The strongest anatase peak occurs at a 2θ value of 25.39° and the strongest rutile peak at 27.51°. The proportion of rutile increased at higher reactor temperatures (Figure 4). At lower temperatures TiO_2 molecules form clusters that coalesce to form anatase crystals. At higher temperatures the transformation of anatase to rutile becomes energetically favorable which leads to increase in the rutile content of the powders. This transformation is initiated by the formation of rutile nuclei on the surface of anatase particles followed by the growth of rutile toward the interior: high defect concentration leads to faster transformation rates (Mackenzie, 1975). Suyama et al. (1975) observed a linear increase in rutile content as the reactor temperature was increased, but Morooka et al. (1987) and Kobata et al. (1991) reported that rutile weight fraction was at a maximum at 1,273 K and decreased rapidly at both lower and higher temperatures.

Scanning electron microscopy was used to study the morphology of titania particles and validate the particle size measurements obtained from the DMPS. The DMPS provides a versatile means for on-line measurement of particle size distribution free from sampling artifacts or those introduced during sample preparation, but is sensitive to changes in sampling flow rates; hence, the DMPS measurements need to be validated before routine usage of the DMPS in characterizing titania particles. Figure 5 shows a typical micrograph of titania particles. At all temperatures investigated, the particle morphology remained the same: dense polyhedral structures. Similar shapes were observed by Suyama and Kato (1976). Size distributions obtained from digitizing scanning electron mi-

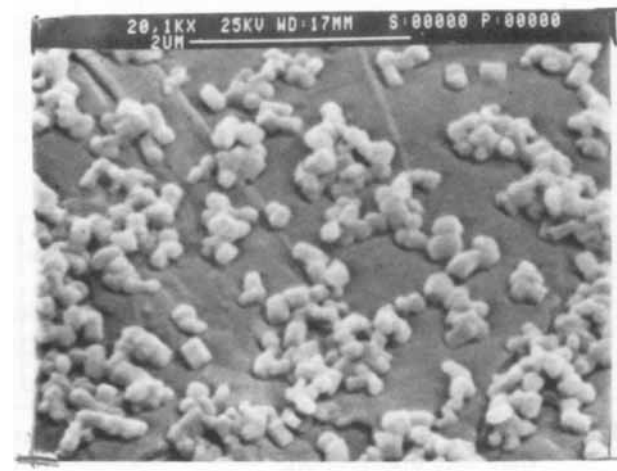

Figure 5. Scanning electron micrograph of titania particles produced at 1,400 K, $TiCl_4$ loading of 1.16×10^{-5} mol/L, and residence time of 1.6 s.

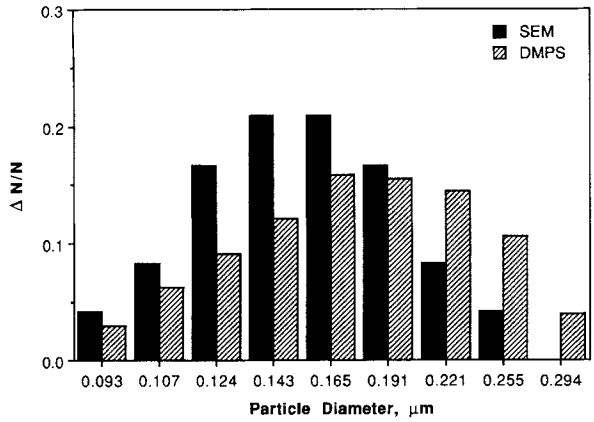

Figure 6. Size distributions: from image analysis of SEM micrographs vs. from the DMPS for particles produced at 1,400 K, $TiCl_4$ loading of 1.16×10^{-5} mol/L and residence time of 1.6 s.

crographs were compared with those obtained from the DMPS. At a reactor temperature of 1,600 K, $TiCl_4$ concentration of 1.16×10^{-5} mol/L and residence time of 1.6 s, the geometric number average particle diameter from microscopy was 0.21 μm and that obtained from the DMPS was 0.24 μm; at 1,400 K a size of 0.18 μm was obtained from microscopy, while the size obtained from DMPS was 0.21 μm (Figure 6). It is observed that the average sizes and the distributions are in reasonably good agreement, though the distributions from microscopic

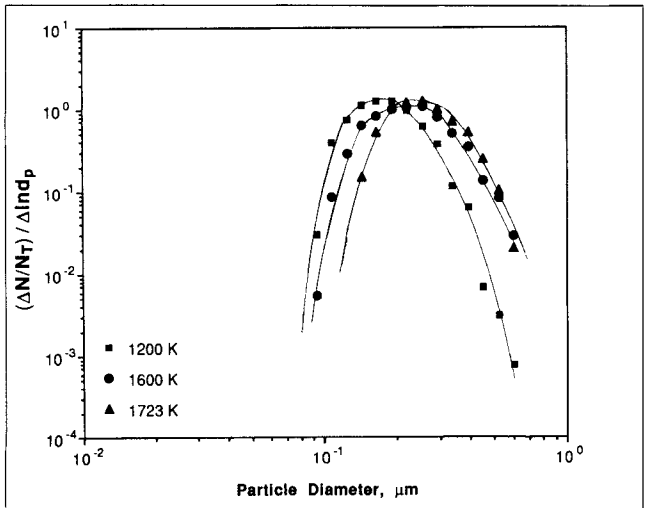

Temperature (K)	Dilution Argon Flow (l/min)	Geometric Number Mean Particle Size (μm)	Geometric Standard Deviation	Total Number Concentration (#/cm³)
1200	2.96	0.18	1.34	1.3×10^7
1600	2.13	0.24	1.38	8.2×10^6
1723	2.02	0.26	1.34	6.9×10^6

Figure 7. Effect of increasing temperature on titania particle size distribution.

$TiCl_4$ concentration was maintained at 1.16×10^{-5} mol/L and the residence time in the isothermal reaction zone was between 1.5 and 1.6 s. The variation in the reported particle diameters was ± 0.02 μm.

measurements are biased toward the smaller sizes. The close agreement between the sizes measured by the DMPS and those obtained from image analysis of the micrographs indicate that in the aerosol phase, titania particles are single dense particles and not chain agglomerates.

Figure 7 shows titania size distributions at 1,200, 1,600 and 1,723 K at an initial $TiCl_4$ concentration of 1.16×10^{-5} mol/L. The flow of dilution argon was varied between 2.02 and 2.96 L/min to maintain constant both residence time and concentration of $TiCl_4$ entering the reaction zone. Nitrogen gas flow rate in the primary dilutor was maintained at 5 L/min, and a stream of 150 cm³/min was withdrawn from the dilutor effluents and mixed with 23 L/min of air in the secondary dilutor prior to DMPS measurements. The geometric number average diameter of the particles increases from 0.18 μm at 1,200 K to 0.26 μm at 1,723 K. At higher temperatures, a higher concentration of TiO_2 monomers is obtained through a higher reaction rate that increases the collision frequency and leads to an increase in the size of the particles generated. Though significant changes in the mean particle size are seen with increasing temperature, the shape of the distribution does not change and the geometric standard deviation is around 1.4. Comparing the mass of the measured titania size distribution to the mass of incoming $TiCl_4$ and assuming complete conversion, it was found that about 20% of the particles (by mass) were lost on the walls of the reactor, dilutor and sampling tubes.

Formenti et al. (1972) observed that the size of TiO_2 particles produced by burning $TiCl_4$ in an oxygen-hydrogen flame increased with increasing flame temperature. At 1,900 K the diameter of the particles was 0.023 μm and at 3,000 K it was 0.036 μm. Suyama and Kato (1976) have observed that the size of titania particles produced from the oxidation of $TiCl_4$ decreases from 0.68 μm at 1,123 K to 0.3 μm at 1,373 K. It is possible that they obtained these results because their data were based on the $TiCl_4$ concentration at the reactor inlet temperature. If the reaction zone is at a higher temperature than the inlet, then the $TiCl_4$ concentration actually decreases due to gas expansion and this leads to a decrease in the observed particle size. Moreover, keeping the total flow constant based on inlet conditions means that the residence time also decreases due to the expansion of gases at higher temperature. This will further tend to decrease particle size. Suyama and Kato (1976) obtained their size distribution data from microscopic analysis of samples obtained downstream of the reactor. It is possible that at high temperatures their size distribution was skewed by higher thermophoretic losses of the particles on the cooler walls of the manifold and sampling lines.

Figure 8 shows the change in size distribution of the TiO_2 particles generated with increase in $TiCl_4$ concentration in the gas phase. The flow of carrier argon through $TiCl_4$ was varied between 150 and 320 cm³/min, and the dilution argon flow was kept constant at 2.5 L/min. The oxygen flow was set between 24 and 56 cm³/min equivalent to ten times the stoichiometric amount. The size distributions in Figure 8 correspond to a furnace temperature of 1,400 K. It is observed that the geometric mean diameter of the particles increases with increasing $TiCl_4$ vapor concentration. At the large excess of oxygen used, changes in oxygen partial pressure had no effect on the particle size distribution. At high $TiCl_4$ vapor concentration more titanium dioxide is produced resulting in enhanced

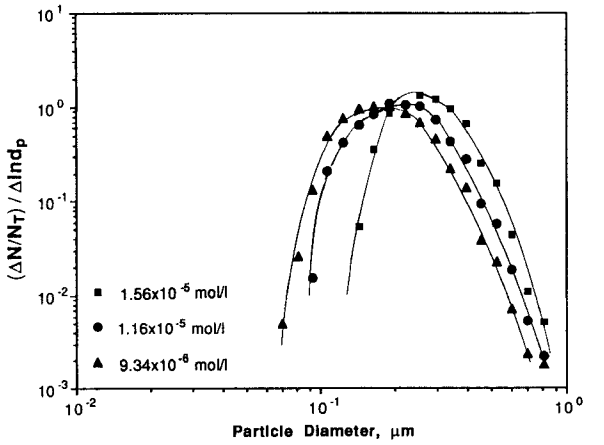

$TiCl_4$ Concentration (mol/l)	Geometric Volume Mean Particle Size (μm)	Geometric Standard Deviation	Total Number Concentration (#/cm³)
1.56×10^{-5}	0.26	1.34	1.2×10^{7}
1.16×10^{-5}	0.21	1.42	1.1×10^{7}
9.34×10^{-6}	0.18	1.44	1.0×10^{7}

Figure 8. Effect of different initial $TiCl_4$ concentration on the average particle size at a temperature of 1,400 K, dilution argon flow of 2.5 L/min, and reactor residence time of 1.6 s.

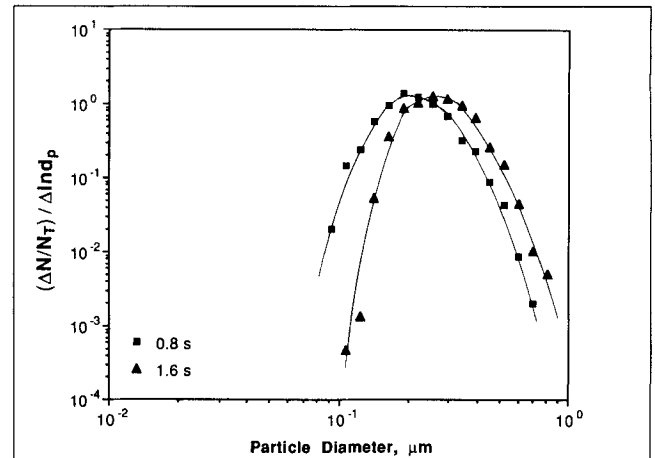

Residence Time (s)	Dilution Argon Flow (l/min)	Geometric Number Mean Diameter (μm)	Geometric Standard Deviation	Total Particle Number Concentration (#/cm³)
0.8	4.5	0.21	1.42	1.4×10^{7}
1.6	2.5	0.27	1.34	1.2×10^{7}

Figure 9. Effect of changing residence time on the particle size distribution at 1,400 K and initial $TiCl_4$ concentration of 1.56×10^{-5} mol/L.

The residence time was varied by changing the flow rate of dilution argon. The error in average particle size measurement was ±0.02 μm.

coagulation and larger particles. From the data accompanying Figure 8 it is evident that increasing the $TiCl_4$ concentration affects particle size more than number concentration. Since coagulation controls particle growth, any increase in $TiCl_4$ concentration primarily serves to increase the mean particle size. The shape of the size distribution does not change, and the geometric standard deviation of the particle distribution remains between 1.34 and 1.44. These numbers indicate that the distributions have attained a self-preserving form by the time they exit the reaction zone (Landgrebe and Pratsinis, 1989). Formenti et al. (1972) observed that in the oxygen-hydrogen flame at 1,900 K the average diameter of the particles increased from 0.0095 to 0.023 μm when they increased the $TiCl_4$ flow rate from 5.56×10^{-4} to 2.86×10^{-2} g/s. Suyama and Kato (1976) and Morooka et al. (1987) also report that particle size increases with increasing $TiCl_4$ loading. Toyama et al. (1990), however, found that titania particles did not show any changes in size with increasing inlet $TiCl_4$ partial pressure. These results are affected most likely by incomplete conversion of $TiCl_4$ at the low temperatures (1,073–1,173 K) investigated.

Figure 9 shows the effect of reactor residence time on the particle size distribution. The $TiCl_4$ concentration and the temperature were kept constant, and the residence time was varied by changing the flow rate of dilution argon into the reactor. The flow of carrier argon through the bottle containing $TiCl_4$ was adjusted to account for these changes. The data are shown for a reactor temperature of 1,400 K and residence times of 1.6 and 0.8 s; dilution argon flow rate was set at 2.5 and 4.5 L/min, the flow of carrier argon was at 305 and 410 cm^3/min, and the oxygen flow rate was 55 and 86 cm^3/min, respectively. The $TiCl_4$ concentration at the entrance of the reaction zone was thus maintained at 1.56×10^{-5} mol/L. As the residence time is increased, the particle size becomes larger and the number concentration decreases. At high residence times the particles produced in the reactor have more time for coagulation, and this leads to larger particles and a decrease in their number.

Figure 10 summarizes the effects of temperature and initial $TiCl_4$ concentration on average particle size at a residence time between 1.5 and 1.6 s. It is observed that the geometric number

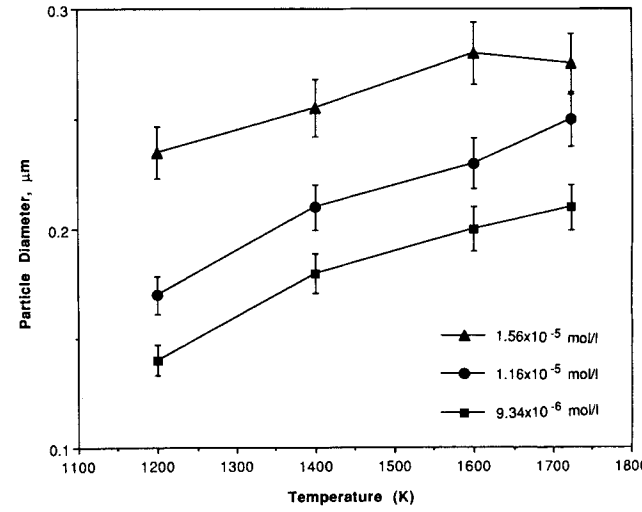

Figure 10. Effect of increasing temperature on the geometric mean particle diameter at different initial $TiCl_4$ concentrations.

The residence time in all cases was between 1.5 and 1.6 s.

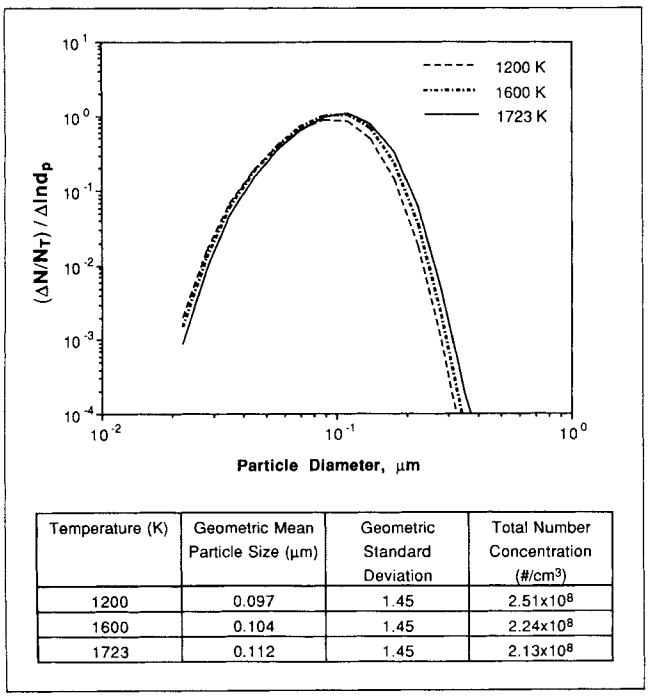

Temperature (K)	Geometric Mean Particle Size (μm)	Geometric Standard Deviation	Total Number Concentration (#/cm³)
1200	0.097	1.45	2.51×10^8
1600	0.104	1.45	2.24×10^8
1723	0.112	1.45	2.13×10^8

Figure 11. Theoretical predictions of the titania particle size distribution at an initial $TiCl_4$ concentration of 1.16×10^{-5} mol/L at different reactor temperatures.

The residence time in the reactor was 1.6 s.

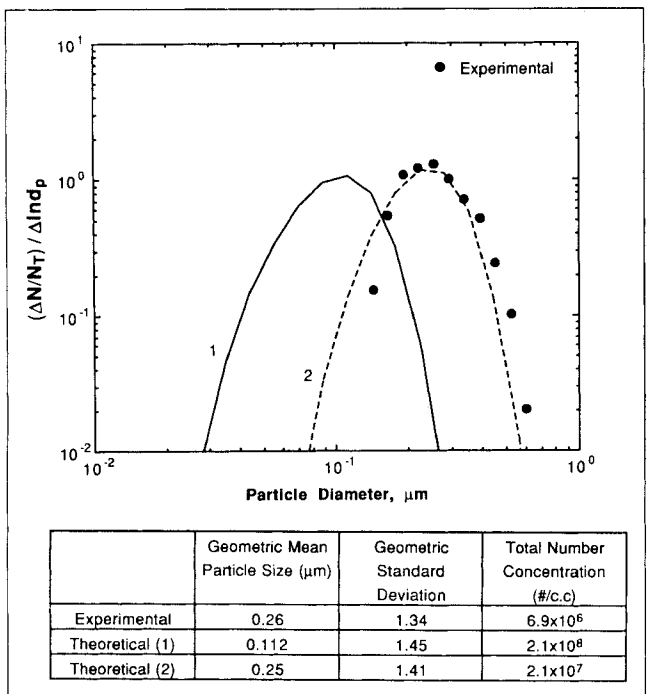

	Geometric Mean Particle Size (μm)	Geometric Standard Deviation	Total Number Concentration (#/c.c)
Experimental	0.26	1.34	6.9×10^6
Theoretical (1)	0.112	1.45	2.1×10^8
Theoretical (2)	0.25	1.41	2.1×10^7

Figure 12. Calculated and experimental size distribution for titania particles at 1,723 K and $TiCl_4$ concentration of 1.16×10^{-5} mol/L.

The residence time was 1.6 s. Curve 1 is the calculated distribution with the coagulation enhancement factor = 1 and curve 2 is with the enhancement factor = 8.3.

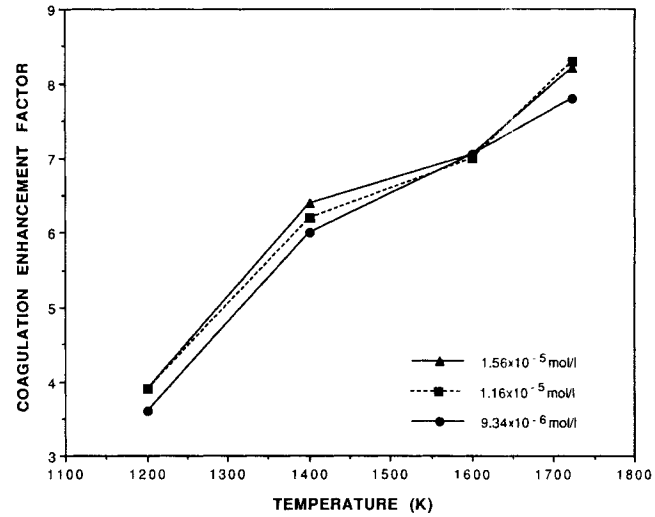

Figure 13. Coagulation enhancement factors as a function of temperature and $TiCl_4$ concentration at a residence time of 1.5 to 1.6 s.

mean particle diameter rapidly increases with increasing temperature at the lower temperatures, but the rate of increase slows down at high temperatures. As $TiCl_4$ concentration is increased, the particle size increases at all the temperatures.

Comparison With Theory

Figure 11 shows the simulation results for the evolution of particle size distribution at 1,200, 1,600 and 1,723 K. $TiCl_4$ concentration was maintained at 1.16×10^{-5} mol/L, and the residence time in the reaction zone was 1.6 s. These conditions correspond to the experimental conditions for the results shown in Figure 7. The size distribution shifts to higher sizes as the temperature is increased, though the shape of the distribution does not change. At higher temperatures the reaction rate increases and a higher amount of titania molecules is available to take part in the coagulation process leading to an increase in the observed particle size. These predictions agree qualitatively with the experimental results of Figure 7, though the effect of temperature predicted by theory is smaller than that observed experimentally.

Figure 12 shows a comparison between the size distributions obtained experimentally and those obtained from simulation at a temperature of 1,723 K. The simulation result predicts a smaller average particle size than that observed experimentally. Excellent agreement between experimental results and theoretical predictions is obtained, if an enhancement factor is employed in the calculation of coagulation rates. The coagulation enhancement factor depends on temperature: at 1,200 K it is 3.9, at 1,400 K it is 6.2, at 1,600 K it is 7, and at 1,723 K it is 8.3 at a $TiCl_4$ concentration of 1.16×10^{-5} mol/L and a residence time of 1.6 s. These enhancement factors remain unaffected by changes in inlet $TiCl_4$ concentration (Figure 13). At 1,400 K and a $TiCl_4$ concentration of 1.16×10^{-5} mol/L the enhancement factor was essentially unaffected by changes in residence time. Okuyama et al. (1984) have shown that interparticle forces like van der Waals forces can greatly enhance particle coagulation. For silver particles in the size range 10 to 20 nm and $Kn = 20$, they found an enhancement fac-

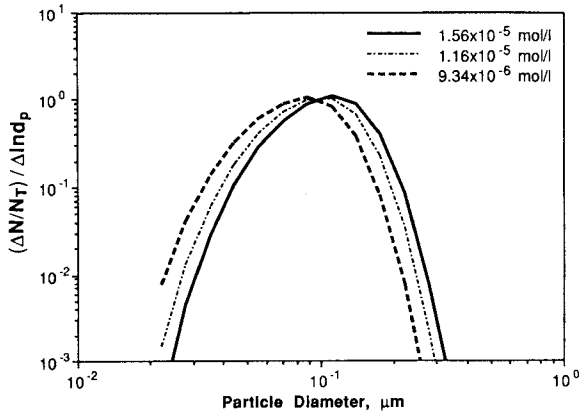

$TiCl_4$ Concentration (mol/l)	Geometric Mean Particle Size (μm)	Geometric Standard Deviation	Total Number Concentration (#/cm³)
$1.56x10^{-5}$	0.121	1.45	$2.18x10^8$
$1.16x10^{-5}$	0.104	1.45	$2.24x10^8$
$9.34x10^{-6}$	0.092	1.47	$2.29x10^8$

Figure 14. Theoretical predictions for the effect of changing initial $TiCl_4$ concentration on the particle size distribution at a temperature of 1,400 K and residence time of 1.6 s.

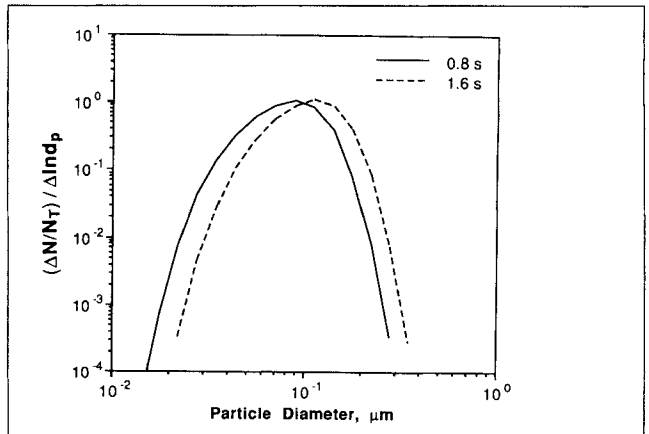

Residence Time (s)	Geometric Mean Particle Size (μm)	Geometric Standard Deviation	Total Number Concentration (#/cm³)
0.8	0.086	1.47	$4.57x10^8$
1.6	0.121	1.45	$2.18x10^8$

Figure 15. Theoretical predictions for the effect of increasing residence time on the particle size distribution at 1,400 K and initial $TiCl_4$ concentration of 1.56×10^{-5} mol/L.

tor ≈ 9. In the early stages of titania particle formation, no doubt, the particles are extremely small (of the order of molecular dimensions) and higher Knudsen numbers exist. While interparticle forces and the nonspherical shape of the particles can explain accelerated coagulation and particle growth, they do not account for the increase in the coagulation enhancement factor with temperature. The effect of van der Waal forces decreases with temperature (Friedlander, 1977) and particle densification is faster at higher temperatures (Kobata et al., 1991). Electron micrographs (Figure 5) reveal that the particle morphology does not change between the temperatures of 1,200 K and 1,723 K, indicating that sintering or particle densification is not rate-limiting at the residence times employed at these temperatures. When the temperature is increased, however, the mean free path of the gas molecules increases so particle growth up to about half a micron in diameter predominantly takes place in the free-molecular regime. Okuyama et al. (1984) have demonstrated that it is in this high Knudsen number regime that coagulation is enhanced the most. In the free molecular and transition regimes, the mass transfer rate on agglomerate particles is inversely proportional to the particle mobility: for the larger particles formed at the higher temperatures, mass transfer is higher resulting in enhanced growth for irregular particles compared to spherical ones (Rogak et al., 1991). It is more difficult to account for the differences in the particle number concentration as they are more sensitive to dilution errors and wall losses. It should be noted that the experimental and theoretical geometric standard deviations were around 1.4 for the most part.

In Figure 14, the effect of changing the initial $TiCl_4$ concentration on the particle size distribution is shown at a temperature of 1,400 K. The shape of the distribution does not change much at the exit of the reactor though the size of the particles increases with increase in $TiCl_4$ concentration. Higher mass loadings lead to higher particle concentrations and result in faster particle growth. These results predict the trends observed in the experimental results of Figure 8.

Increasing the residence time leads to an increase in the particle size. The simulation results for changes in size distribution with increasing residence time at 1,400 K are shown in Figure 15. It is observed that the size distribution shifts to higher particle sizes, as the residence time is increased from 0.8 s to 1.6 s. The experimental results of Figure 9 are in agreement with these predictions. The sectional model predicts the trends in particle growth observed experimentally though numerically precise predictions of the enhanced particle growth need to take into account interparticle forces, shape factor, diffusive losses to the walls, and the detailed flow patterns inside the reactor.

Conclusions

The production of TiO_2 particles by the vapor-phase oxidation of $TiCl_4$ was studied experimentally, and the effect of process variables was investigated. Changes in temperature, reactant concentration, and residence time allowed control of particle size distribution. The geometric number average particle diameter ranged from 0.13 μm to 0.35 μm with a standard deviation of about 1.4. The close agreement between the sizes obtained from the DMPS and the image analysis of the micrographs indicated that the particles were not chain-like agglomerates, but polyhedral dense structures. From X-ray diffraction analysis, it was found that the titania particles were primarily anatase and that the transformation to the rutile phase was accelerated with increasing temperature. The geometric number average particle diameter increased with temperature; increasing the initial $TiCl_4$ concentration or reactor

residence time led to consistent increase in the size of the particles. These experimental observations are in qualitative agreement with theoretical predictions obtained through solving the aerosol general dynamic equation for chemical reaction and coagulation by a sectional technique. Excellent quantitative agreement between experimental data and theoretical predictions is obtained when a coagulation enhancement factor is employed.

Acknowledgment

This research was supported by the National Science Foundation, Grant CTS-8908197 and E. I. DuPont de Nemours. The authors acknowledge stimulating discussions with P. Biswas (University of Cincinnati) and S. V. R. Mastrangelo (DuPont).

Notation

A = Avogadro's number, 6.02×10^{23} #/mol
c = precursor vapor concentration, mol/g
$c(0)$ = initial precursor vapor concentration, mol/g
E = reaction activation energy, kJ/mol
k_1 = chemical reaction rate constant, 1/s
Kn = Knudsen number
n_i = number concentration of titania particles, #/m^3
R = gas constant, 8.314 J/mol/K
t = time, s
T = temperature, K

Greek letters

β = coagulation coefficient, m^3/s
σ = geometric standard deviation of particle number distribution

Literature Cited

Bowen, H. K., "Basic Research Needs on High-Temperature Ceramics for Energy Applications," *Matt. Sci. Eng.*, **44**, 1 (1980).

Clark, H. B., "Titanium Dioxide Pigments," *Treatise on Coatings: Pigments: 3*, P. R. Myers and J. S. Long, eds., Marcel Dekker, New York (1977).

Formenti, M., F. Juillet, P. Meriaudeau, S. J. Teichner, and P. Vergnon, "Preparation in a Hydrogen-Oxygen Flame of Ultrafine Metal Oxide Particles," *Aerosols and Atmospheric Chemistry*, G. M. Hidy, ed., Academic Press, New York (1972).

Friedlander, S. K., *Smoke, Dust and Haze*, Wiley, New York (1977).

Gelbard, F., Y. Tambour, and J. H. Seinfeld, "Sectional Representations for Simulating Aerosol Dynamics," *J. Colloid Interf. Sci.*, **76**, 541 (1980).

George, A. P., R. D. Murley, and E. R. Place, "Formation of TiO_2 Aerosol from the Combustion Supported Reaction of $TiCl_4$ and O_2," *Farad. Symp. Chem. Soc.*, **7**, 63 (1973).

Juillet, F., F. Lecomte, H. Mozzanega, S. J. Teichner, A. Thevenet, and P. Vergnon, "Inorganic Oxide Aerosols of Controlled Submicronic Dimensions," *Farad. Symp. Chem. Soc.*, **7**, 57 (1973).

Kingery, W. D., H. K. Bowen, and D. R. Uhlmann, *Introduction to Ceramics*, Chap. Wiley, New York. (1976).

Kobata, A., K. Kusakabe, and S. Morooka, "Growth and Transformation of TiO_2 Crystallites in Aerosol Reactor," *AIChE J.*, **37**, 347 (1991).

Landgrebe, J. D., and S. E. Pratsinis, "Gas-Phase Manufacture of Particulates: Interplay of Chemical Reaction and Aerosol Coagulation in the Free-Molecular Regime," *I&EC Res.*, **28**, 1474 (1989).

Landgrebe, J. D., and S. E. Pratsinis, "A Discrete-Sectional Model for Particulate Production by Gas-Phase Chemical Reaction and Aerosol Coagulation in the Free-Molecular Regime," *J. Colloid Interf. Sci.*, **139**, 63 (1990).

Mackenzie, K. J. D., "The Calcination of Titania: V. Kinetics and Mechanism of the Anatase-Rutile Transformation in the presence of Additives," *Trans. J. Brit. Ceram. Soc.*, **74**, 77 (1975).

Morooka, S., T. Yasutake, A. Kobata, K. Ikemizu, and Y. Kato, "Mechanism of TiO_2 Fine Particle Formation by Gas-Phase Reaction," *Kagaku Kogaku Ronbunshu*, **13**, 159 (1987); English translation in *Int. Chem. Eng.*, **29**, 119 (1989).

Okuyama, K., Y. Kousaka, and K. Hayashi, "Changes in Size Distribution of Ultrafine Aerosol Particles Undergoing Brownian Coagulation," *J. Colloid Interf. Sci.*, **101**, 98 (1984).

Pratsinis, S. E., H. Bai, P. Biswas, M. Frenklach, and S. V. R. Mastrangelo, "Kinetics of $TiCl_4$ Oxidation," *J. Amer. Ceramic Soc.*, **73**, 2158 (1990).

Rice, R. W., "Ceramic Processing: an Overview," *AIChE J.*, **36**, 481 (1990).

Rogak, S. N., U. Baltensperger, and R. C. Flagan, "Measurement of Mass Transfer to Agglomerate Aerosols," *Aerosol Sci. and Technol.*, **14**, 447 (1991).

Spurr, R. A., and H. Myers, "Quantitative Analysis of Anatase-Rutile Mixtures with an X-Ray Diffractometer," *Analytical Chem.*, **29**, 760 (1957).

Suyama, Y., and A. Kato, "TiO_2 Produced by Vapor-Phase Oxygenolysis of $TiCl_4$," *J. Amer. Ceramic Soc.*, **59**, 146 (1976).

Suyama, Y., K. Ito, and A. Kato, "Mechanism of Rutile Formation in Vapor Phase Oxidation of $TiCl_4$ by Oxygen," *J. Inorg. Nucl. Chem.*, **37**, 1883 (1975).

Toyama, S., M. Nakamura, H. Mori, K. Kanai, and T. Nachi, "The Production of Ultrafine Particles by Vapor Phase Oxidation from Chlorine," *Proc. World Cong. Particle Tech.*, Kyoto, Japan, 360 (1990).

Ulrich, G. D., "Theory of Particle Formation and Growth in Oxide Synthesis Flames," *Comb. Sci. Technol.*, **4**, 47 (1971).

Xiong, Y., and S. E. Pratsinis, "Gas-Phase Production of Particles in Reactive Turbulent Flows," *J. Aerosol Sci.*, **22**, in press (1991).

Manuscript received May 20, 1991, and revision received Aug. 26, 1991.